Computational Biology and Chemistry 120 (2026) 108681

Contents lists available at ScienceDirect

Computational Biology and Chemistry

journal homepage: www.elsevier.com/locate/cbac

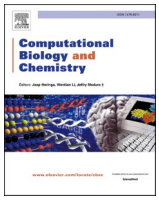

Development and validation of a breast cancer survival prediction model based on perioperative anesthesia-related drug target genes and analysis of immune microenvironment and drug sensitivity

Dongmei Yu [a,1,2], Jiajia Li [a,1,2], Wenjing Ma [a], Yue Pei [a], Yingchao Qi [e], Tong Yu [a], Wenkai Li [f], Xiaohan Sun [a], Jingyan Zhang [e], Xuantonghe Li [a], Longyan Liang [a], Yunen Liu [a,b,c,d,*], Yichen Wang [a,b,c,d,*]

[a] School of Shuren International, Shenyang Medical College, Shenyang, Liaoning Province 110141, China
[b] School of Innovation and Entrepreneurship, Shenyang Medical College, Shenyang, Liaoning Province 110141, China
[c] Liaoning Provincial Key Laboratory of Skin, Mucosa and Soft Tissue Trauma Repair and Reconstruction, China
[d] Shenyang Municipal Key Laboratory of Digestive System Injury Repair and Reconstruction, Shenyang, Liaoning Province, China
[e] Liaoning University of Traditional Chinese Medicine, Shenyang, Liaoning Province 110031, China
[f] Yanshan University, Qinhuangdao, Hebei Province, China

ARTICLE INFO

Keywords:
Breast cancer
Perioperative anesthesia-related drug target genes (PARDTGs)
Survival prediction model
Immune microenvironment
Drug sensitivity

ABSTRACT

Introduction: This study aimed to create a survival prediction model for breast cancer(BC) using perioperative anesthesia - related drug target genes(PARDTGs). It explored their immune microenvironment and drug sensitivity for personalized therapy.

Methods: Transcriptomic sequencing data of BC were downloaded from The Cancer Genome Atlas (TCGA) database. Common PARDTGs were retrieved from the DrugBank and ChemBL databases. Transcriptomic data were analyzed to identify differentially expressed PARDTGs (DE-PARDTGs) using rigorous statistical thresholds. A total of 101 machine learning algorithms were applied to construct PARDTG-based survival prediction models. Patients were stratified into high- and low-risk groups based on model-derived risk scores. Model performance was validated using an independent dataset from the Gene Expression Omnibus (GEO). Clinical-pathological correlations, immune profiling, and mutational landscapes were compared between risk groups in the TCGA-BRCA cohort. Drug sensitivity to commonly used therapies was predicted via transcriptomic correlations.

Results: We identified five DE - PARDTGs (PTGS2, TACR1, ADRB1, ABCB1, ACKR3) for a BC prognostic model. Receiver Operating Characteristic - Area Under the Curves (ROC - AUCs) for 1 -, 3 -, 5 - year overall survival(OS) were 0.722, 0.730, 0.691. TACR1 and ADRB1 high - expression meant better prognosis. Risk groups differed in immunity, with TACR1 correlating with immune checkpoints and drug sensitivity. Conclusions: The PARDTG - based model predicts BC survival independently. TACR1, key to immune response and drug sensitivity, could be a new therapeutic target. These results stress the importance of focusing on perioperative anesthesia - related drug targets in BC research.

1. Introduction

Breast cancer(BC) is one of the most prevalent malignancies among women worldwide, with persistently high incidence and mortality rates. According to the latest statistics, the number of newly diagnosed breast cancer cases globally has exceeded that of lung cancer, making it the most common cancer (Bashar and Begam, 2022). Meanwhile, breast cancer is also a leading cause of cancer-related deaths among women,

* Corresponding authors at: School of Shuren International, Shenyang Medical College, Shenyang, Liaoning Province 110141, China.
E-mail addresses: yudongmei1@hotmail.com (D. Yu), 2992533923@qq.com (J. Li), mawenjing223@gmail.com (W. Ma), yuepei810@gmail.com (Y. Pei), qi_yingchao@sina.com (Y. Qi), tongy9179@gmail.com (T. Yu), 526314160@qq.com (W. Li), sunxiaohan0503@163.com (X. Sun), 1134264861@qq.com (J. Zhang), 3531447699@qq.com (X. Li), 2720254693@qq.com (L. Liang), lye9901@163.com (Y. Liu), yichenwang@yeah.net (Y. Wang).
[1] These authors contributed equally.
[2] Co-first authors

https://doi.org/10.1016/j.compbiolchem.2025.108681
Received 10 July 2025; Received in revised form 27 August 2025; Accepted 8 September 2025
Available online 16 September 2025

accounting for 15 % of all cancer-related fatalities (Global Burden of Disease Cancer et al., 2019). Treatment modalities for breast cancer include surgery, radiotherapy, chemotherapy, endocrine therapy, and immunotherapy. The vast majority of patients undergo surgical procedures. In recent years, an increasing number of studies have demonstrated that perioperative events influence the risk of cancer recurrence, and the use of drugs such as β-agonists and intravenous anesthetics during the perioperative period is associated with patient prognosis (Hiller et al., 2017). Therefore, perioperative anesthesia management is not only crucial for patients' short-term recovery but also merits attention for its potential impact on long-term prognosis. In recent years, research has revealed that perioperative anesthesia-related drugs may not only affect the physiological state of patients during the perioperative period, thereby influencing the biological behavior of cancer cells (Wall et al., 2019), but may also act on specific target pathways or regulate the expression of certain genes, affecting the biological behavior of breast cancer and potentially impacting patient prognosis (Inada et al., 2011; Kwakye et al., 2020; Yang et al., 2017). This makes the potential role of anesthesia in breast cancer treatment an important yet understudied area.

Previous studies have shown that perioperative anesthesia-related drugs such as sevoflurane (Deng et al., 2020; Kim et al., 2023), propofol (Wang et al., 2020b), and midazolam (Lu et al., 2021) may influence cancer progression by affecting the proliferation, apoptosis, invasion, and drug resistance of cancer cells, regulating the tumor microenvironment, or modulating the immune system (Kadantseva et al., 2024). However, there is a paucity of research on the expression changes and clinical significance of perioperative anesthesia-related drug target genes (PARDTGs) in breast cancer, especially their specific roles in breast cancer progression and prognosis. Additionally, perioperative anesthesia typically involves the combined use of multiple drugs, and studies on individual anesthetics may not fully elucidate the comprehensive impact of anesthesia on breast cancer patients. In contrast, the target genes of commonly used perioperative anesthesia-related drugs may play a more extensive and sustained role in the occurrence and development of breast cancer. Therefore, exploring these genes can provide deeper insights into the potential impact of anesthesia on breast cancer.

In this study, we utilized PARDTGs in combination with breast cancer transcriptomic and genomic data to screen for differentially expressed genes and construct a risk model for predicting patient prognosis. We analyzed the expression of these genes and their associations with clinical outcomes, aiming to explore their roles in the development, personalized treatment, and prognosis prediction of breast cancer. This research not only offers a new perspective for precision medicine in breast cancer but also provides evidence for the potential impact of anesthesia on breast cancer treatment. The analysis flowchart is shown in Fig. 1.

2. Methods

2.1. Clinical samples and data collection

Transcriptome sequencing data of breast cancer patients from The Cancer Genome Atlas database (TCGA,https://www.cancer.gov/ccg/research/genome-sequencing/tcga) were downloaded using the TCGAbiolinks package in R software (Version 4.3.2). Perioperative anesthesia-related drug target genes (PARDTGs) were identified from the DrugBank database (https://go.drugbank.com/) and Chembl database (https://www.ebi.ac.uk/chembl/). External validation datasets GSE1456 and GSE45827 were downloaded from the Gene Expression Omnibus (GEO, https://www.ncbi.nlm.nih.gov/geo/) using the GEOquery package.

2.2. Identification of differentially expressed PARDTGs

Transcriptome sequencing data were processed and normalized. Differential expression analysis was performed using the DESeq2 package in R to screen for significantly differentially expressed genes (DEGs) with a threshold of $|\log_2 \text{fold change (FC)}| > 1$ and $p < 0.05$. An intersection was taken between PARDTGs and all DEGs to extract differentially expressed PARDTGs. The pheatmap package was used to generate volcano plots, heatmaps, and Venn diagrams to visualize the expression patterns and screening results of differentially expressed genes.

2.3. GO and KEGG enrichment analysis

GO (Gene Ontology) and KEGG (Kyoto Encyclopedia of Genes and Genomes) enrichment analyses were conducted using the clusterProfiler package in R, with a significance threshold of $p < 0.05$. The top 20 enriched terms were selected and visualized via circle plots, chord diagrams, and correlation plots to present the results.

2.4. Screening of key genes and construction of prognostic model

Survival information of breast cancer patients was downloaded from the UCSC Xena official website (https://xena.ucsc.edu/). Survival data were integrated with the expression levels of 48 commonly used perioperative anesthesia-related drug target genes (PARDTGs) identified in this study. The "Mime1" package in R was used to construct prognostic models using 101 machine learning methods, with the following specific steps:1.Key gene screening: Five key genes significantly associated with survival were selected from 48 PARDTGs via univariate Cox proportional hazards regression analysis.2.Model construction: Prognostic models were developed using the 101 machine learning methods based on the five key genes, and risk scores were generated.3.Model evaluation: The grouping ability of the risk model was assessed via Kaplan-Meier (K-M) survival curves and log-rank tests.4.External validation: The GEO cohort was used as an independent validation set to further verify the model's reliability.5.Model performance assessment: Time-dependent receiver operating characteristic (ROC) curves for one-year, three-year and five-year survival were plotted using the "survival" and "timeROC" packages in R, and the area under the curve (AUC) was calculated to evaluate the model's predictive performance.

2.5. Screening of core genes and external validation

The R package "Mime1" was used for further screening of core genes. Box plots of core gene expression levels between normal and tumor groups were plotted, and the expression of core genes was validated using GEO datasets (https://www.ncbi.nlm.nih.gov/geo/). Protein expression levels of core genes were verified on the UALCAN(The University of ALabama at Birmingham CANcer) website (https://ualcan.path.uab.edu/analysis.html).

2.6. Construction of nomogram

Clinical information was downloaded from the UCSC Xena official website (https://xena.ucsc.edu/). Univariate and multivariate Cox regression analyses were performed on clinical information and risk scores using the "survival" package to evaluate the independent predictive ability of risk scores. Nomograms were constructed using the "rms" package in R by integrating significant factors from multivariate Cox regression analysis to predict the one-year, three-year, and five-year overall survival of breast cancer patients.

2.7. Clinical correlation analysis

Clinical data of breast cancer (BC) patients were integrated to analyze differences in risk scores across different clinical characteristic

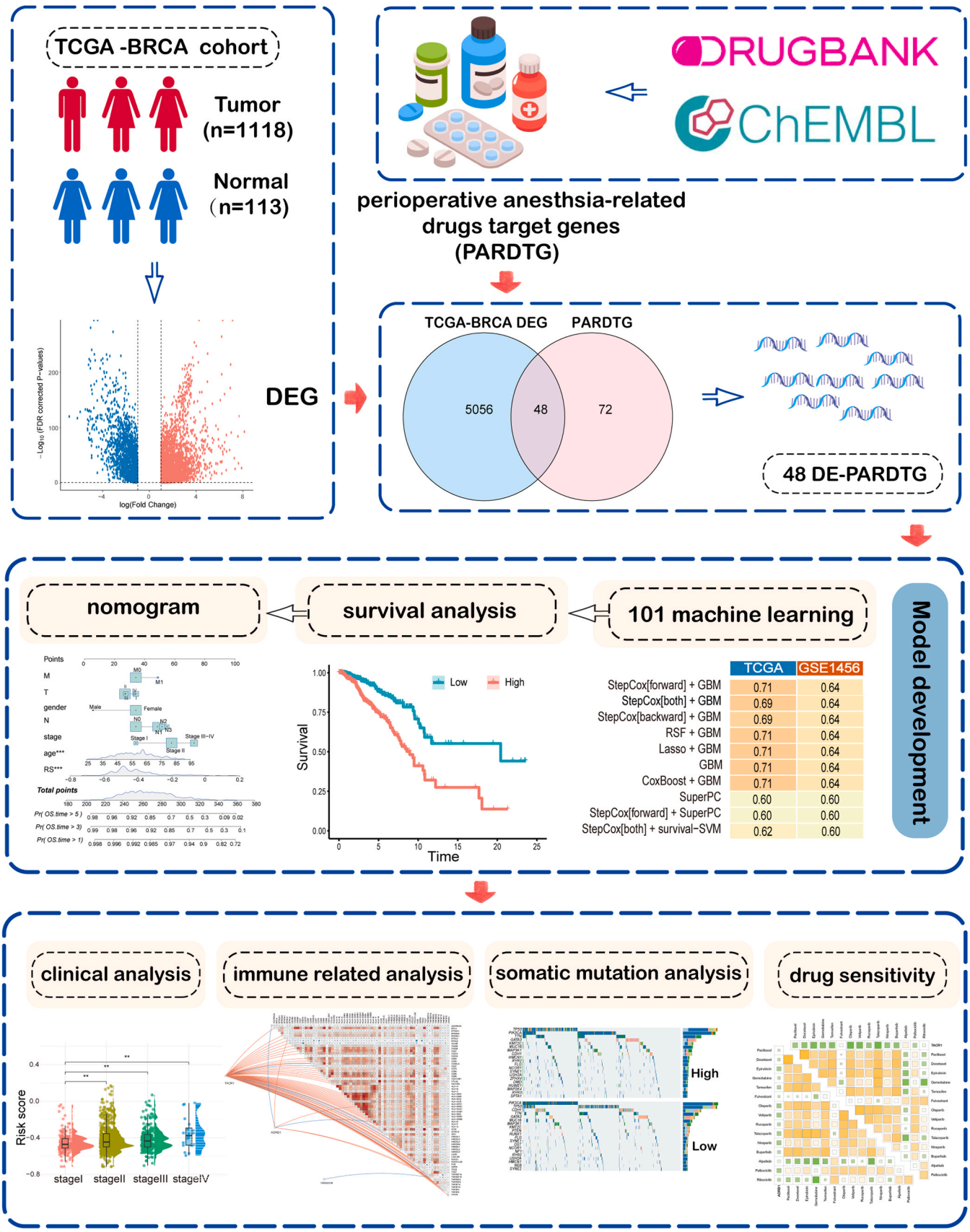
TCGA -BRCA cohort
Tumor (n=1118)
Normal (n=113)
DEG
DRUGBANK
ChEMBL
perioperative anesthsia-related drugs target genes (PARDTG)
TCGA-BRCA DEG
PARDTG
5056
48
72
48 DE-PARDTG
nomogram
survival analysis
101 machine learning
Model development
Low
High
Survival
Time
TCGA
GSE1456
StepCox[forward] + GBM 0.71 0.64
StepCox[both] + GBM 0.69 0.64
StepCox[backward] + GBM 0.69 0.64
RSF + GBM 0.71 0.64
Lasso + GBM 0.71 0.64
GBM 0.71 0.64
CoxBoost + GBM 0.71 0.64
SuperPC 0.60 0.60
StepCox[forward] + SuperPC 0.60 0.60
StepCox[both] + survival-SVM 0.62 0.60
clinical analysis
immune related analysis
somatic mutation analysis
drug sensitivity
Risk score
stageI
stageII
stageIII
stageIV
High
Low

Fig. 1.

groups. Chi-square tests were used to compare the distribution of clinical characteristics between high-risk and low-risk groups. Raincloud plots and heatmaps were generated using the ComplexHeatmap package in R, while stacked plots were created with the "ggplot2" and "RColorBrewer" packages.

2.8. Immune-related analysis

Immune cell infiltration analysis was performed using the Xcell and Cibersort algorithms via the "IBOR" package in R, with the following steps:

1) Data normalization: Results of immune infiltration analysis were normalized.

2) Difference comparison: Immune infiltration differences were compared between normal and tumor tissues, high-risk vs. low-risk groups, and high vs. low expression groups of TACR1 and ADRB1 genes.

3) Visualization Box plots were plotted using ggplot2. Mantel tests were conducted on TACR1, ADRB1, risk scores, and immune checkpoint genes using the "vegan" package, followed by butterfly plot visualization. Wilcoxon rank-sum tests were used to compare immune checkpoint gene expression between high-and low-risk groups, with lollipop plots generated via "ggplot2".

2.9. Genomic mutation profiling analysis

Mutation annotation format (MAF) data of breast cancer patients were downloaded from the TCGA database using the "TCGAbiolinks" package in R. Genomic mutation characteristics were analyzed with the "maftools" package, and waterfall plots were plotted. Tumor mutational burden (TMB) and mutational allele tumor heterogeneity (MATH) were calculated for survival analysis. Violin plots and survival curves were generated using "ggviolin"and" ggsurvplot", respectively.

2.10. Drug sensitivity analysis

Drug sensitivity analysis was performed using the "oncoPredict" package in R. Drug response data were obtained from the GDSC(Genomics of Drug Sensitivity in Cancer) database and analyzed in conjunction with breast cancer gene expression data, with normalization of the gene expression matrix. The IC50 values (half maximal inhibitory concentration) of samples to different drugs were calculated using built-in functions of "oncoPredict". The ggpubr package and Wilcoxon rank-sum test were used to further compare drug response differences between high-risk and low-risk groups, and box plots were generated. Correlation analysis between core genes (TACR1 and ADRB1) and commonly used clinical drugs was performed and visualized using the "ggplot2" package.

2.11. Statistical Analysis

All statistical analyses were conducted using R software (version 4.3.2 and version4.4.2). $P < 0.05$ was considered statistically significant.

3. Result

3.1. Identification of differentially expressed perioperative anesthesia-related target genes

We downloaded transcriptomic data from 1118 breast cancer samples and 113 normal samples in the TCGA database. To investigate global gene expression differences between normal and tumor samples, differential expression analysis was performed, identifying a total of 5014 differentially expressed genes (DEGs), including 3161 upregulated and 1943 downregulated genes ($|\log_2 FC| => 1$ and $p < 0.05$). Principal component analysis (PCA) of all DEGs was conducted to visualize sample clustering, revealing a clear separation between tumor and normal samples (Fig. 2A). A volcano plot was generated to display DEGs (Fig. 2B).

A total of 120 perioperative anesthesia-related drug target genes (PARDTGs) were identified from the Drugbank (https://go.drugbank.com/) and Pubchem (https://pubchem.ncbi.nlm.nih.gov/) databases based on the types of drugs commonly used in the perioperative period (including sedative-hypnotics, analgesics, etc.) and in combination with clinical guidelines (Supplementary Table 4,5) . An intersection analysis between these 120 PARDTGs and the 5014 DEGs yielded 48 differentially expressed PARDTGs (DE-PARDTGs) (Fig. 2C, Supplementary Table 3). A heatmap was created to visualize the expression patterns of these 48 genes (Fig. 2D).

Further principal component analysis (PCA) was performed using the 48 DE-PARDTGs, and the results (Fig. 2E) showed a significant separation between tumor and normal samples, indicating substantial differences in the expression of these genes between the two groups.

3.2. GO and KEGG analysis

GO and KEGG enrichment analyses were performed on the 48 DE-PARDTGs. GO analysis revealed enrichment of these genes in biological processes (BP), cellular components (CC), and molecular functions (MF) (Fig. 3A). Specifically, they were predominantly enriched in biological processes such as synaptic transmission, monoamine neurotransmitter transport, membrane potential regulation, and ion transmembrane transport. Significant enrichment was also observed in molecular functions including receptor activity, G protein-coupled receptor signaling, and ion channel regulation.

KEGG pathway enrichment analysis showed that these genes were significantly enriched in a series of pathways, including the cAMP signaling pathway, calcium signaling pathway, neuroactive ligand-receptor interaction, nicotine addiction pathway, and angiogenesis-related pathways (Fig. 3B).

3.3. Construction of prognostic model

We employed 101 machine learning methods to develop a prognostic model using the48 DE-PARDTGs in breast cancer. During model construction, univariate regression analysis was first performed to screen five key genes: PTGS2, TACR1, ADRB1, ABCB1, and ACKR3. The prognostic model constructed by the StepCox[both]+GBM method demonstrated optimal performance in both the training and validation sets (Fig. 4A).

Patients in the TCGA-BRCA cohort were stratified into high- and low-risk groups based on the median risk score of this model. Scatter plots of overall survival information showed a significantly higher number of deaths in the high-risk group (Fig. 4B, C). Heatmaps depicting the expression profiles of the five key genes revealed distinct patterns between the two risk groups (Fig. 4D). Kaplan-Meier survival analysis indicated a significant difference in overall survival between high- and low-risk groups ($p < 0.0001$).

Time-dependent receiver operating characteristic (ROC) curves were generated to evaluate model performance, yielding area under the curve (AUC) values of 0.722, 0.730, and0.691 for one-, three-, and five-year survival, respectively, in the TCGA-BRCA cohort (Fig. 4H, I).

External validation in the GSE1456 cohort confirmed consistent results: patients stratified by the same risk model showed higher mortality in the high-risk group (Fig. 4E, F), distinct expression patterns of key genes (Fig. 4G), and significant survival differences ($p < 0.0001$). The AUC values for one-, three-, and five-year survival in the validation cohort were 0.761, 0.641, and 0.663, respectively (Fig. 4J, K).

These results demonstrate the robust performance and clinical applicability of our risk model in predicting breast cancer prognosis across independent cohorts.

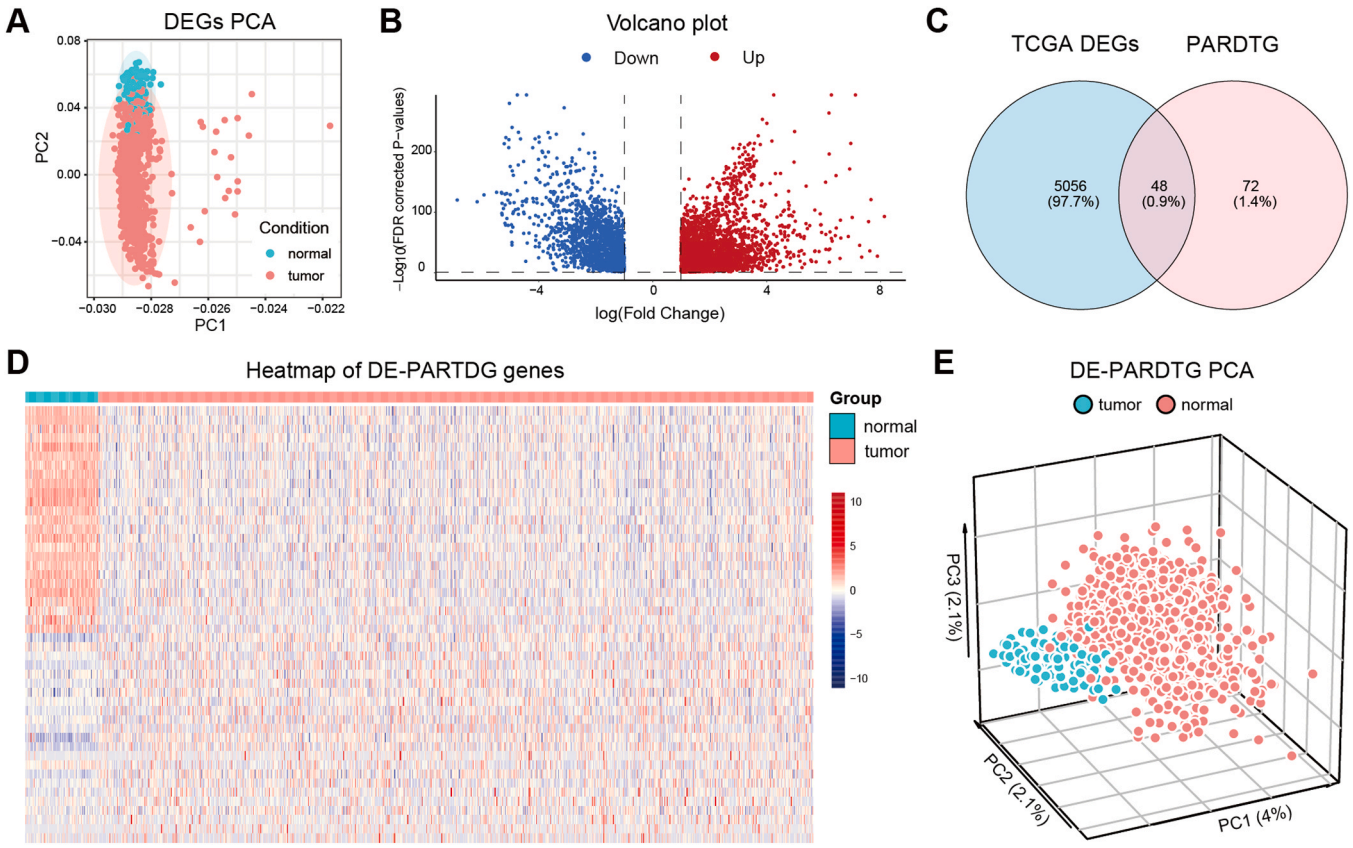

Fig. 2. PCA and differential expression analysis (A) PCA analysis of differentially expressed genes (DEGs). (B) Volcano plot of DEGs. (C) Venn diagram showing the intersection between DEGs in TCGA-BRCA and PARDTGs. (D) Heatmap of differentially expressed PARDTGs. (E) PCA analysis of differentially expressed PARDTGs.

3.4. Screening of core genes

Using 18 bioinformatics tools to screen for core genes, 17 of these methods consistently identified TACR1 and ADRB1 (Fig. 5A). Expression validation of TACR1 and ADRB1 was performed in the GSE45827 cohort. Results showed that both genes were lowly expressed in tumor tissues and highly expressed in normal tissues, consistent with findings from the TCGA cohort. Heatmaps of core gene expression indicated that TACR1 and ADRB1 were both under-expressed in the high-risk group, suggesting that their high expression may be associated with lower tumor incidence and better prognosis (Fig. 4D, G; Fig. 5B, C, F, G). Additionally, protein expression levels of core genes were verified using the UALCAN website. Results showed that TACR1 (also known as SPR) was significantly downregulated in tumor tissues (Fig. 5D).Patients were stratified into high- and low-expression groups based on the median expression levels of TACR1 and ADRB1. Survival analysis revealed that patients in the high-expression groups exhibited significantly longer survival than those in the low-expression groups (Fig. 5E, H). These findings indicate that high expression of TACR1 and ADRB1 is associated with favorable prognosis.

3.5. Nomogram and clinical correlation analysis

Next, we validated the prognostic value of the risk score through univariate (Fig. 6A) and multivariate (Fig. 6B) Cox regression analyses incorporating clinical information. Results demonstrated that the risk score was statistically significant and could serve as an independent prognostic factor. To enhance the efficiency and accuracy of predicting overall survival in breast cancer patients, we developed a clinically applicable nomogram. This nomogram integrates age, gender, tumor stage, and risk score to comprehensively estimate the one-, three-, and five-year survival probabilities of patients (Fig. 6C). Calibration curves were plotted to compare predicted probabilities with actual outcomes, confirming the good predictive performance of the nomogram (Fig. 6D). Using patient survival data, we generated a heatmap integrating risk groups and clinical information to visualize the distribution of survival time, clinical characteristics, and risk stratification. Results showed that patients in the high-risk group had significantly shorter survival times, higher mortality rates, older ages, and a higher proportion of male patients (Supplementary Figure 2). We further investigated whether risk scores differed across age, gender, and tumor stage subgroups, revealing significant associations with age and gender. These findings suggest that certain clinical factors may influence patient prognosis. Additionally, analysis of MKI67 (encoding Ki67) expression in different risk groups showed significantly higher expression in the high-risk group, which may contribute to the poorer prognosis of this subgroup (Fig. 6E). Chi-square test results for clinical characteristic distribution between high- and low-risk groups indicated significant differences in multiple parameters (Fig. 6F). Survival analysis across clinical subgroups (stratified by age, T stage, N stage, M stage, and overall tumor stage) demonstrated that the risk score could significantly distinguish patient outcomes in all subgroups ($P < 0.05$), highlighting its broad applicability and robustness across diverse populations (Supplementary Figure 1).

3.6. Immune infiltration analysis

To analyze the composition and function of immune cells across different groups, we performed immune infiltration analysis on normal and tumor tissues using the XCell algorithm. Results showed that eosinophils, MEP (myeloid erythroid progenitors), mesangial cells, MSCs (mesenchymal stem cells), NKT cells(Natural Killer T cell), osteoblasts, and plasma cells were more abundant in tumor tissues compared to normal tissues. Tumor tissues also exhibited higher ImmuneScore, while normal tissues had significantly higher HSC (hematopoietic stem cell)

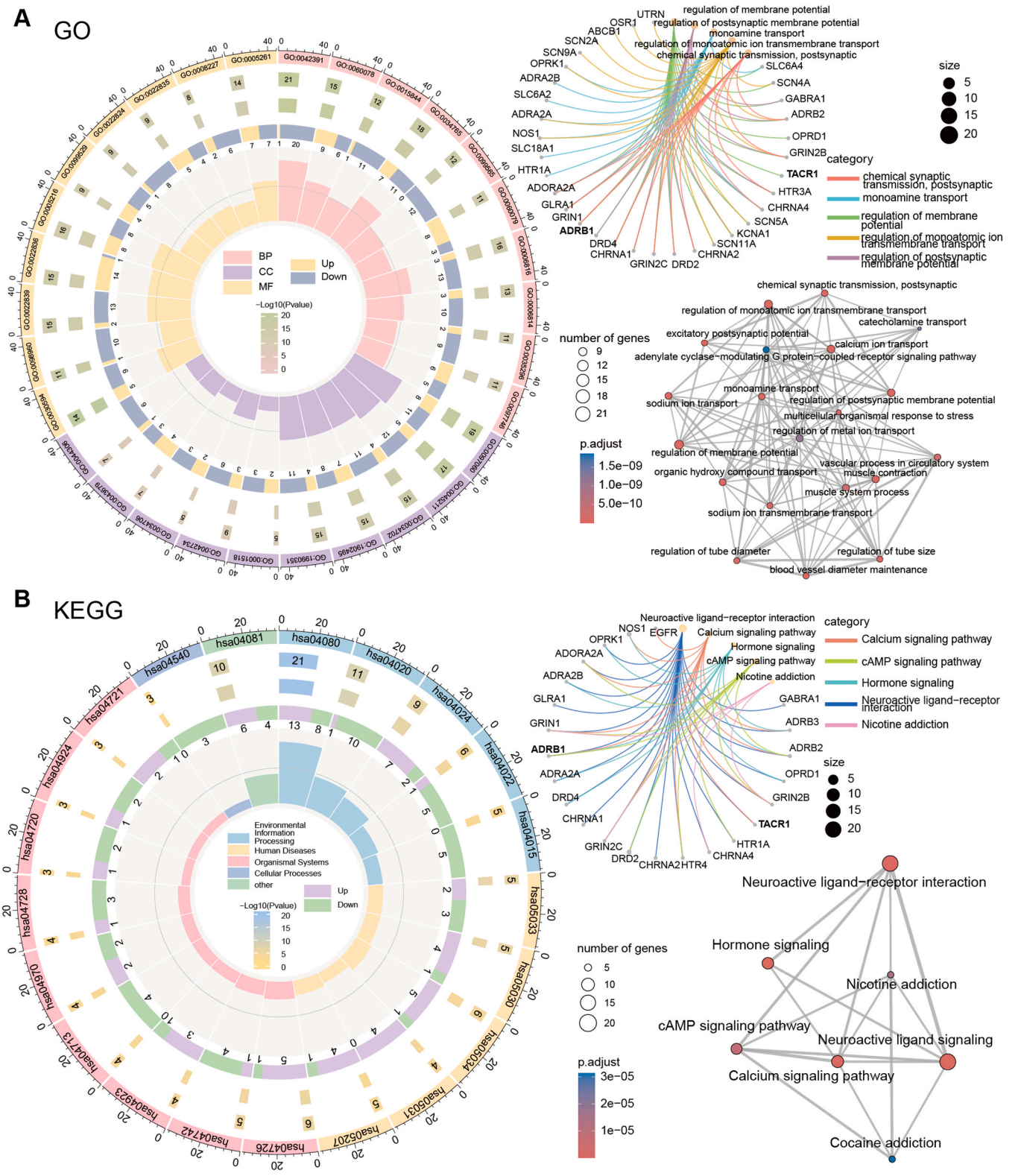

Fig. 3. GO and KEGG enrichment analysis (A) GO enrichment analysis – Circle plots, gene-pathway correlation plots, and pathway-network association diagrams for the top 10 BP (biological processes), CC (cellular components), and MF (molecular functions). (B) KEGG enrichment analysis – Circle plots, gene-pathway correlation plots, and pathway-network association diagrams.

infiltration (Fig. 7A). In immune infiltration analysis of high- and low-risk groups in tumor tissues, MEP, NKT cells, smooth muscle cells, astrocytes, MSCs, and mesangial cells were more abundant in the high-risk group. Conversely, CD4 + Tem (effector memory T cells), CD4 + Tcm (central memory T cells), mast cells, HSCs, class-switched memory B cells, and basophils were more enriched in the low-risk group (Fig. 7B). Cibersort algorithm analysis of tumor immune microenvironment composition between risk groups revealed higher M1 macrophage infiltration in the low-risk group and higher M2 macrophage infiltration in the high-risk group. Stratifying patients into high- and low-expression

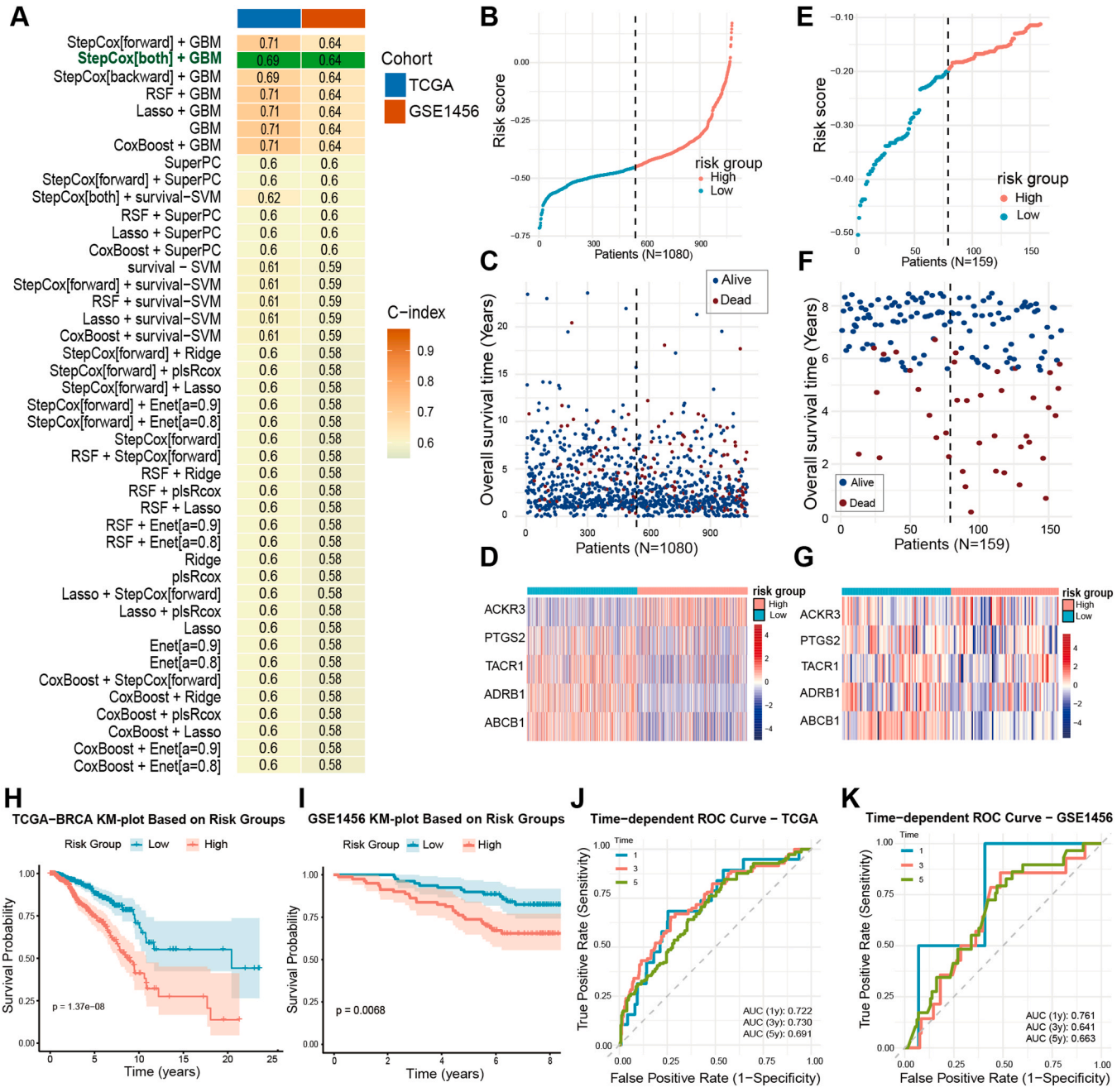

Fig. 4. Construction of the prognostic model (A) Model development using 101 machine learning methods. (B) Distribution of risk scores in the TCGA-BRCA cohort based on the PARDTG-derived model. (C) Survival status of high- and low-risk groups in the TCGA-BRCA cohort based on the DE-PARDTG model. (D) Expression profiles of model-constructed genes in high- and low-risk groups of the TCGA-BRCA cohort. (E) Distribution of risk scores in the GEO cohort based on the PARDTG-derived model. (F) Survival status of high- and low-risk groups in the GEO cohort based on the PARDTG-derived model. (G) Expression profiles of model-constructed genes in high- and low-risk groups of the GEO cohort. (H) Kaplan-Meier survival curves for overall survival (OS) in high- and low-risk groups of the TCGA-BRCA cohort based on the PARDTG-derived model. (I) Time-dependent receiver operating characteristic (ROC) curves for predicting overall survival in the TCGA-BRCA cohort using the PARDTG-derived model. (J) Kaplan-Meier survival curves for OS in high- and low-risk groups of the GEO cohort based on the PARDTG-derived model. (K) Time-dependent ROC curves for predicting overall survival in the GEO cohort using the PARDTG-derived model.

groups based on the median expression levels of TACR1 and ADRB1, we observed similar trends in immune cell composition between the two groups. Specifically, CD4 + Tem, HSCs, and class-switched memory B cells were more abundant in the high-expression groups (Fig. 7C, D), which also showed better prognosis (Fig. 5F, I). This suggests that these immune cells may be associated with favorable outcomes.

3.7. *Immune checkpoint analysis*

Correlation analysis was performed among core genes TACR1, ADRB1, risk scores, and immune checkpoint genes (Fig. 8A). Results showed significant correlations between TACR1 and common immune checkpoint genes such as BTLA, CTLA-4, and PDCD1, indicating that TACR1 may interact with immune checkpoint genes to influence tumor development and progression, thereby affecting prognosis. Expression of immune checkpoint genes was compared between high- and low-risk

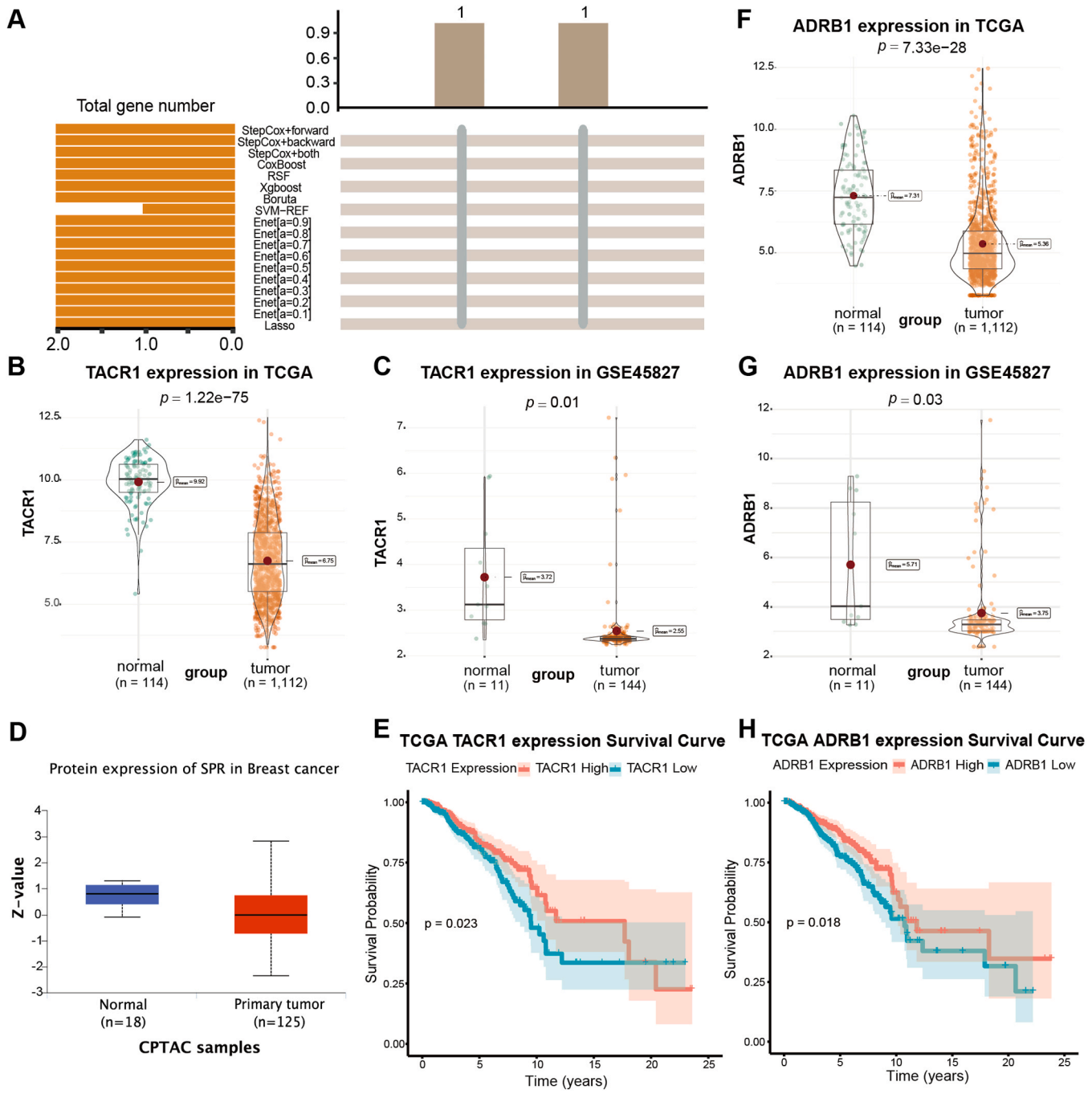

Fig. 5. Screening and external validation of core genes (A) Screening of core genes using machine learning methods. (B) Expression of TACR1 in normal and tumor tissues of the TCGA-BRCA cohort.(C) Expression of TACR1 in normal and tumor tissues of the GEO cohort.(D) Protein expression of TACR1 (SPR) in normal and tumor tissues analyzed via UALCAN.(E) Kaplan-Meier survival curves for high- vs. low-expression groups of TACR1 in the TCGA-BRCA cohort.(F) Expression of ADRB1 in normal and tumor tissues of the TCGA-BRCA cohort.(G) Expression of ADRB1 in normal and tumor tissues of the GEO cohort.(H) Kaplan-Meier survival curves for high- vs. low-expression groups of ADRB1 in the TCGA-BRCA cohort.

groups. Multiple common checkpoint genes including BTLA, CTLA-4, and PDCD1 were significantly upregulated in the low-risk group ($P < 0.0001$). This may be associated with the better prognosis of the low-risk group, suggesting that patients in the low-risk group are more likely to benefit from immunotherapy (Fig. 8B).

3.8. *Genomic mutation profiling analysis*

Genomic variability analysis was performed on MAF(Mutation Annotation Format) data of TCGA-BRCA. First, mutation profiles were compared between high- and low-risk groups, revealing distinct mutational patterns. In the high-risk group, 450 out of 516 samples (87.21 %) had mutations, with the top three mutated genes being TP53, PIK3CA, and TTN, primarily involving frameshift deletions and missense mutations. In the low-risk group, 417 out of 474 samples had mutations, with the top three genes being PIK3CA, TP53, and CDH1, mainly characterized by missense and nonsense mutations (Fig. 9A). Subsequently, genes with significantly different mutation frequencies between risk groups were analyzed (Fig. 9B). PTPRD and BRCA2 exhibited higher mutation rates in the high-risk group (OR<1, $p < 0.01$), while CDH1 was more

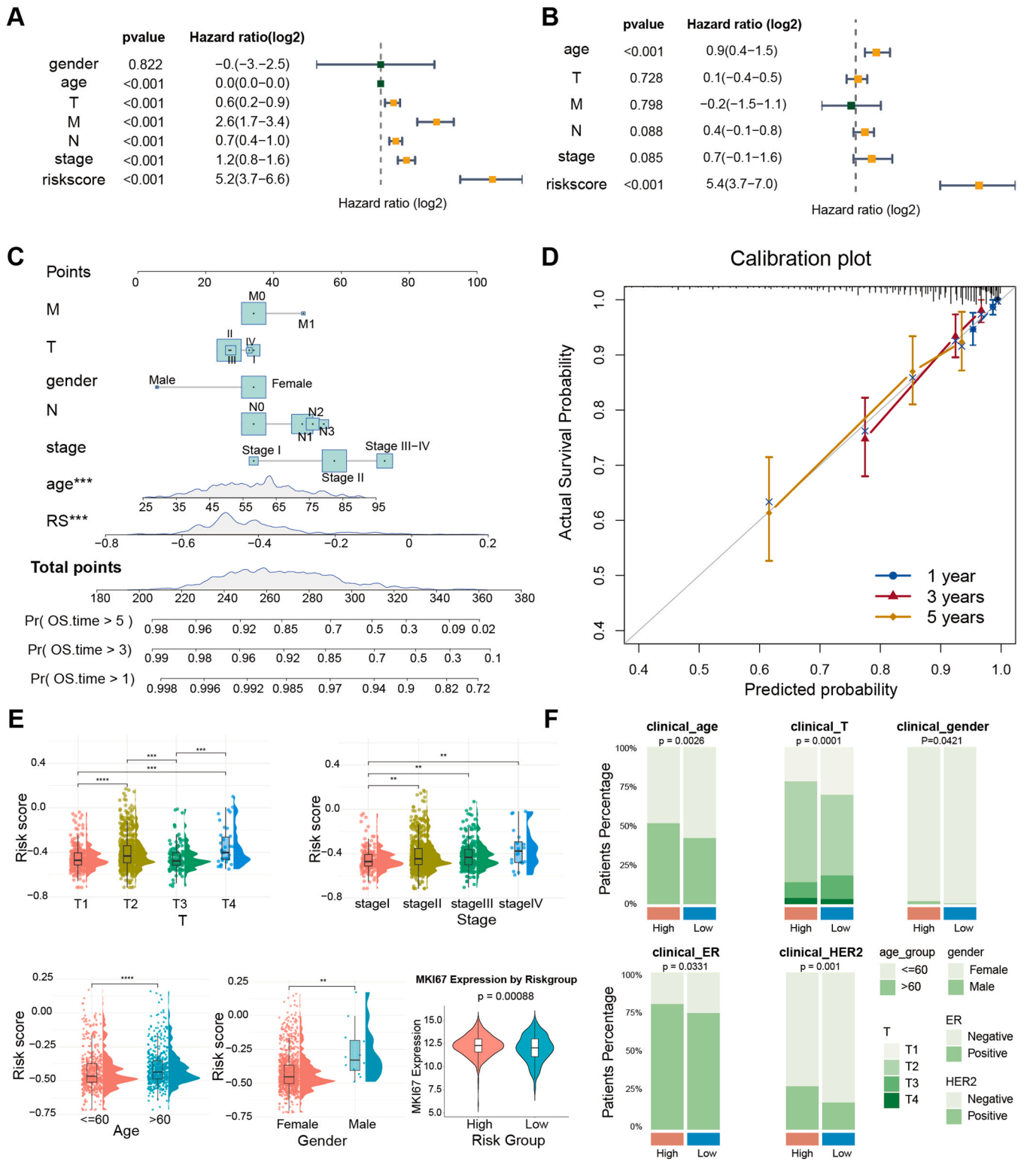

Fig. 6. Construction of the nomogram (A) Univariate regression analysis. (B) Multivariate regression analysis. (C) Nomogram integrating risk scores based on five PARDTGs and clinical characteristics. (D) Calibration plot of actual risk probabilities. (E) Raincloud plots of risk scores across clinical subgroups and MKI67 gene expression between high/low-risk groups. (F) Bar charts showing the distribution of clinical characteristics between high-and low-risk groups.

frequently mutated in the low-risk group. This suggests that CDH1 may be closely associated with favorable prognosis. Analysis of tumor mutational burden (TMB) revealed significant differences between risk groups, with the high-risk group showing higher TMB (Fig. 9C). Stratifying patients by the optimal TMB cutoff value, the low-TMB group demonstrated better survival outcomes (Fig. 9D). Similarly, mutational allele tumor heterogeneity (MATH) was significantly higher in the high-risk group (Fig. 9C). Patients with high MATH had poorer prognosis compared to low-MATH counterparts (Fig. 9D).

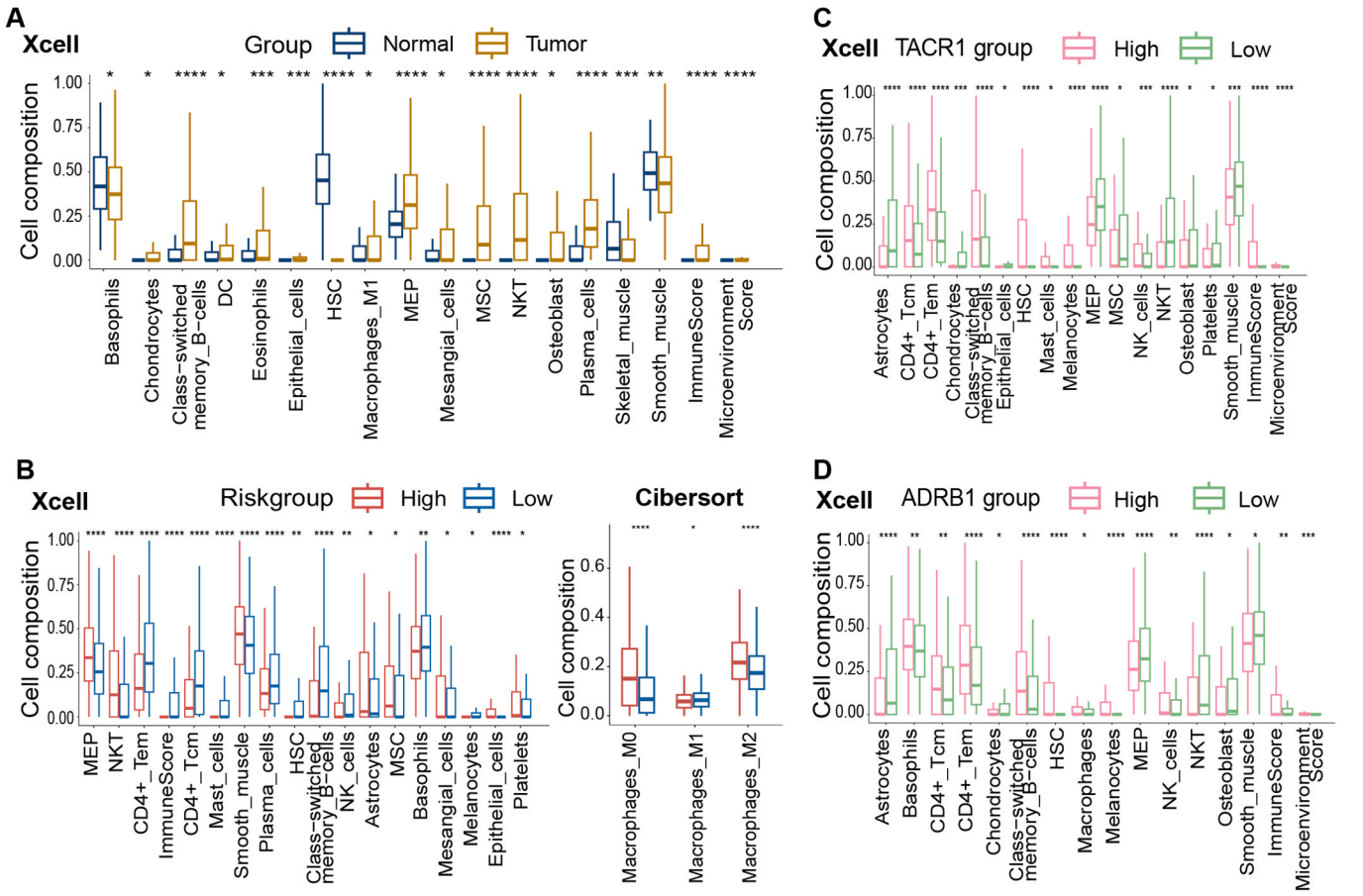

Fig. 7. Immune infiltration analysis (A) Differences in immune infiltration between normal and tumor tissues in the TCGA-BRCA cohort. (B) Differences in immune infiltration between high- and low-risk groups based on the PARDTG-derived model in the TCGA-BRCA cohort. (C) Differences in immune infiltration between high- and low-expression groups of TACR1 in the TCGA-BRCA cohort.(D) Differences in immune infiltration between high- and low-expression groups of ADRB1 in the TCGA-BRCA cohort. *P < 0.05, **P < 0.01, ***P < 0.001, ****P < 0.0001.

3.9. Drug sensitivity analysis

Drug sensitivity prediction analysis was performed on patients in the TCGA-BRCA cohort. Fifteen commonly used drugs for breast cancer treatment with significant therapeutic effects were selected, and their sensitivity was compared between high- and low-risk groups. Results showed significant differences in drug sensitivity between the two groups. The low-risk group generally exhibited lower IC50 values, indicating higher sensitivity to these therapeutic drugs (Fig. 10A). In the TCGA-BRCA cohort, patients were stratified into high- and low-expression groups based on the median expression levels of core genes TACR1 and ADRB1 for drug sensitivity analysis. Notably, TACR1 low-expression groups showed significantly higher sensitivity to Alpelisib and Fulvestrant, while TACR1 high-expression groups were more sensitive to the remaining 13 drugs. For ADRB1, high-expression groups demonstrated higher sensitivity to all drugs except Alpelisib, with significant differences observed in sensitivity to 14 drugs compared to low-expression groups (Fig. 10B). Correlation analysis between TACR1/ADRB1 expression levels and responses to the 15 drugs revealed: TACR1 expression was positively correlated with Alpelisib, Fulvestrant, and Ribociclib (higher expression → higher IC50 → lower sensitivity) and negatively correlated with all other drugs (higher expression → lower IC50 → higher sensitivity). ADRB1 expression was negatively correlated with all drugs except Alpelisib (higher expression → lower IC50 → higher sensitivity) (Fig. 10C).

4. Discussion

Breast cancer(BC) is one of the most common malignancies among women worldwide, with its incidence and mortality rates consistently ranking among the highest. Surgery is a common treatment for breast cancer, and the majority of patients require surgical intervention. Perioperative events can influence patient prognosis to some extent, making the impact of perioperative anesthesia-related medications worthy of attention. These medications may regulate the biological behavior of breast cancer through their target genes, thereby affecting patient outcomes. Despite the complex and diverse types of perioperative anesthetic drugs, most existing studies focus on the potential effects of specific anesthetics on breast cancer. Our study aimed to construct a risk prediction model by investigating the target genes of commonly used perioperative anesthesia-related drugs, thereby predicting breast cancer prognosis from a novel perspective and exploring the potential roles of these genes in tumorigenesis, development, and prognosis.

We identified 48 differentially expressed perioperative anesthesia-related drug target genes (DE-PARDTGs) in breast cancer, which were significantly enriched in pathways such as cAMP signaling, calcium signaling, neuroactive ligand-receptor interaction, nicotine addiction, and angiogenesis.Among them, cAMP can promote cancer cell growth, and can also inhibit cell proliferation and survival under specific conditions (H. Zhang et al., 2024). The cAMP/PKA/CREB pathway has been shown to act as a downstream signaling pathway of JAK/STAT3 to promote chemoresistance in inflammatory breast cancer, while PKA-mediated inhibition of ERK1/2 may enhance the sensitivity of triple-negative breast cancer cells to doxorubicin (Yu et al., 2017a).

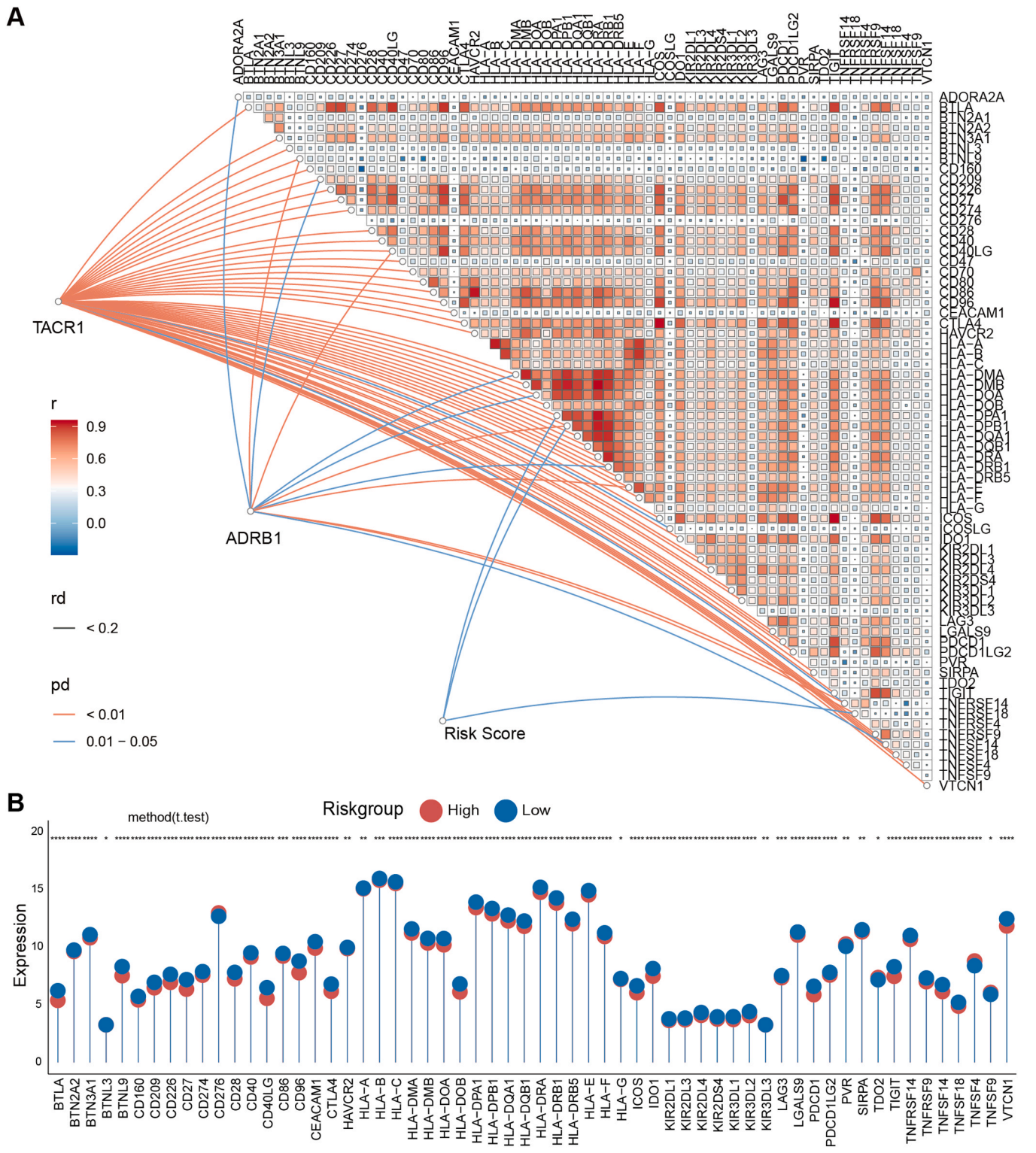

Fig. 8. Immune checkpoint analysis (A) Correlations among core genes TACR1, ADRB1, risk scores, and immune checkpoint genes in the TCGA-BRCA cohort. (B) Expression of immune checkpoint genes in high- and low-risk groups based on the PARDTG-derived model in the TCGA-BRCA cohort. *P < 0.05, **P < 0.01, ***P < 0.001, ****P < 0.0001.

Studies have shown that calcium signaling can regulate many immune-related processes in cancer, modulate immune checkpoints, reshape the tumor microenvironment, and is associated with reverse multidrug resistance and inhibition of immune escape (L. Wu et al., 2021).In the nicotine addiction pathway, nicotine promotes dopamine (DA) release by activating nicotinic acetylcholine receptors (nAChRs) in the central nervous system. Studies have shown that this process can activate downstream pathways such as JAK2/STAT3 and PI3K/Akt, thereby promoting the proliferation, migration, and anti-apoptotic ability of breast cancer cells (Guha et al., 2014). Additionally, nicotine increases the proportion of breast cancer stem-like cells, enhancing tumor drug resistance and metastatic potential.Angiogenesis is a critical

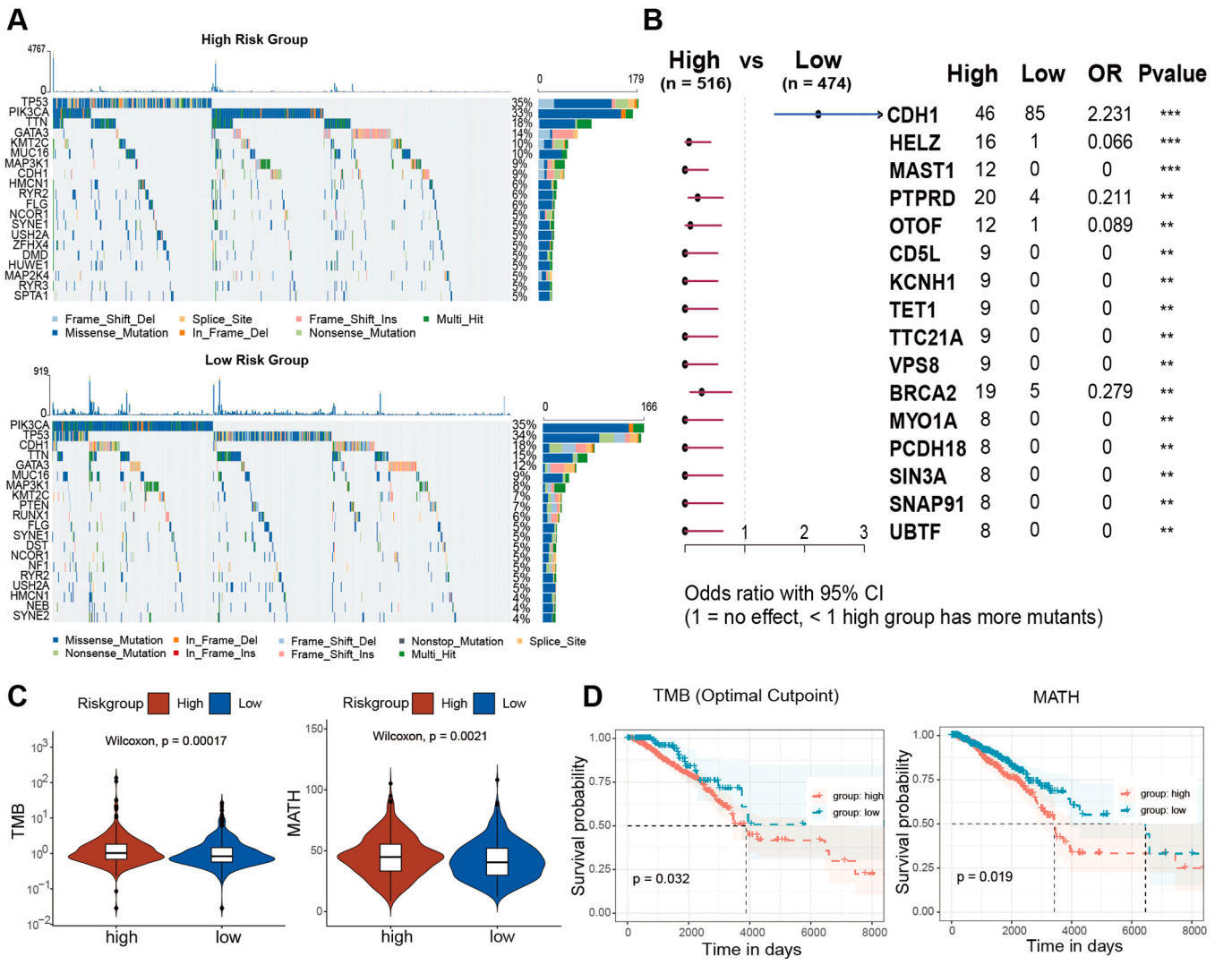

Fig. 9. Genomic variation analysis (A) Distribution of the top 20 mutated genes in high- and low-risk groups of TCGA-BRCA. (B) Forest plot of the most significantly differentially mutated genes between high- and low-risk groups. (C) Analysis of TMB and MATH in high- and low-risk groups. (D) Kaplan-Meier survival curves for high- and low-TMB/MATH groups. *P < 0.05, **P < 0.01, ***P < 0.001, ****P < 0.0001.

process for the growth and spread of solid tumors (Ayoub et al., 2022). These pathways highlight the key roles of our studied PARDTGs in the development and prognosis of breast cancer.

Using univariate regression analysis, we identified five perioperative anesthesia-related drug target genes(PARDTGs) significantly associated with prognosis: PTGS2, TACR1, ADRB1, ABCB1, and ACKR3. A risk model was constructed using these five genes. Existing studies have highlighted the critical role of TACR1 in tumorigenesis and prognosis: In neuroblastoma, TACR1 has been identified as a potent anticancer target across various neuroblastoma subtypes (Pohl et al., 2017). In head and neck squamous cell carcinoma, TACR1 methylation serves as a novel biomarker (Misawa et al., 2013). Full-length neurokinin-1 (encoded by TACR1) expression is negatively correlated with tumor lymph node metastasis (TNM stage) and lymph node metastasis, indicating its role in breast cancer prognosis (Zhou et al., 2019). ADRB1 has been recognized as a prognostic biomarker in breast cancer (Li and Liu, 2021). ADRB1 mutations are associated with lower tumor mutational burden (TMB), and patients with such mutations exhibit better clinical outcomes (Wang, 2020a). PTGS2 plays a key role in breast cancer biology: it has been identified as a gene influencing paclitaxel treatment response (J. Wu et al., 2021), and its activation and overexpression may promote breast cancer metastasis and drug resistance, thereby affecting prognosis (Festa-Vasconcellos et al., 2012). ABCB1 gene polymorphisms are associated with breast cancer susceptibility (Madrid-Paredes et al., 2020), and ABCB1 is linked to paclitaxel and doxorubicin resistance in breast cancer cell lines (Fultang et al., 2020; Wang et al., 2023; D. Zhang et al., 2023), influencing prognosis. ACKR3 regulates breast cancer metastasis (Stacer et al., 2016), and its high expression is associated with poorer overall survival (OS) (Yang et al., 2023), consistent with our findings. These results validate the role of these genes in cancer and breast cancer development and prognosis, confirming the reliability of our screening results.

Analysis of immune infiltration between normal and tumor groups revealed higher ImmuneScore and more abundant immune cell infiltration in tumor tissues, indicating immunological changes during breast cancer progression. Immune infiltration analysis of high- and low-risk groups showed similar compositions but distinct quantities of immune cells in the microenvironment. The high-risk group was enriched in MEP(myeloid progenitor cells),NKT(Nature Killer T cell), and MSCs (mesenchymal stem cells), while the low-risk group had higher proportions of CD4 + Tem(effector memory T cells), CD4 + Tcm(central memory T cells),mast cells, HSCs(hematopoietic stem cells),class-switched memory B cells, and basophils.

In the high-risk group, the enrichment of cells such as MEP, NKT, and MSC may be associated with the formation of a highly aggressive tumor and an immunosuppressive microenvironment. The enrichment of MEP

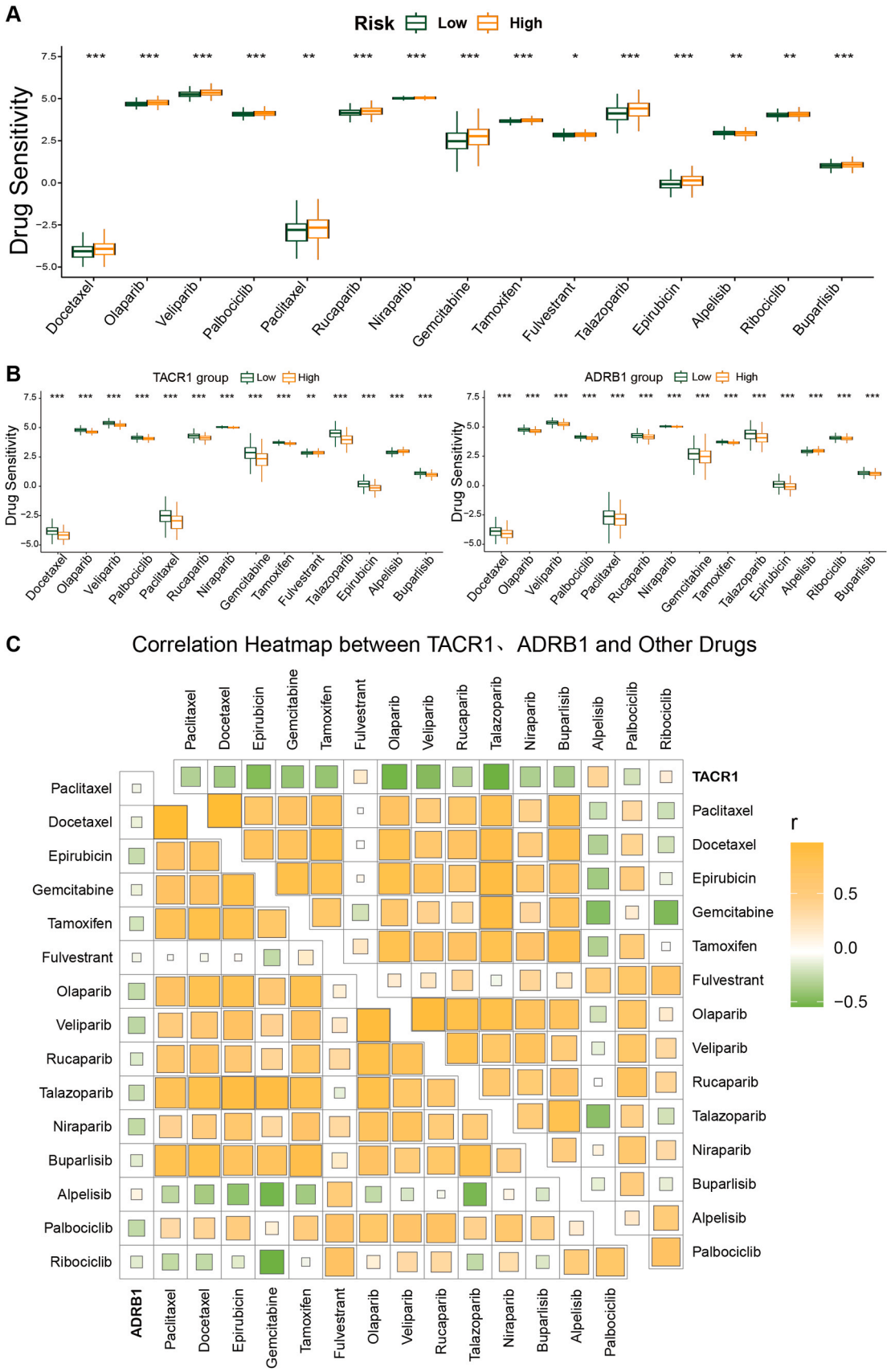

Fig. 10. Drug sensitivity analysis (A) Box plots showing differences in drug sensitivity between high- and low-risk groups based on the PARDTG-derived model in the TCGA-BRCA cohort. (B) Box plots showing differences in drug sensitivity between high-/low-expression groups of TACR1 and ADRB1 in the TCGA-BRCA cohort. (C) Correlation heatmap between TACR1, ADRB1, and commonly used clinical therapeutic drugs. *P < 0.05, **P < 0.01, ***P < 0.001, ****P < 0.0001.

(myeloid progenitor cells) may indicate abnormal proliferation of myeloid cells, which can be altered in the tumor microenvironment to exert pro-inflammatory and immunosuppressive effects (Gabrilovich et al., 2012).NKT cells have dual roles in anti-tumor immunity, potentially exerting immunosuppressive effects when induced by the tumor microenvironment (Tyznik et al., 2014).MSCs (mesenchymal stem cells) are closely associated with immunosuppression. They inhibit CD8 + T cell function and promote Treg cell proliferation by secreting immunosuppressive factors (e.g., PGE2, IDO), thereby fostering an immunosuppressive microenvironment that facilitates tumor growth (Shi et al., 2017).

In the low-risk group, cells may exhibit more active anti-tumor immunity, with CD4 + Tem (effector memory CD4 + T cells) and CD4 + Tcm (central memory CD4 + T cells) playing crucial roles in tumor immunity.CD4 + Tcm cells provide long-term immune memory and rapidly differentiate into effector T cells upon antigen stimulation, while CD4 + Tem cells mediate rapid effector responses. This suggests stronger immune memory and adaptive immune responses in the low-risk group. CD4 + T cells can directly kill tumor cells or indirectly inhibit tumors by activating innate immune cells or reducing tumor angiogenesis (Kravtsov et al., 2022). Class-switched memory B cells were significantly increased in the low-risk group, indicating a protective role of humoral immunity. These cells produce isotype-switched antibodies in the tumor microenvironment, which correlate with better prognosis in breast cancer patients, enhance responses to PD-1/PD-L1 immunotherapy, and promote anti-tumor immunity through antigen presentation and T cell activation (Conejo-Garcia et al., 2023; Engelhard et al., 2021; Tsou et al., 2016). This aligns with our immune checkpoint analysis showing that low-risk patients may benefit more from PD-1/PD-L1 therapy. Mast cells have traditionally been recognized as participants in allergic reactions, but recently research indicates their roles in the tumor microenvironment are more complex. In some contexts, mast cells promote tumor progression, whereas in breast cancer, they exhibit protective effects (Varricchi et al., 2017). Previous studies have shown that basophils can infiltrate various human cancers and exert divergent roles in promoting or inhibiting tumorigenesis (Poto et al., 2022). Our study found a higher proportion of basophils in the low-risk group of breast cancer, suggesting a potential protective role of basophils in breast cancer.

Cibersort immune analysis showed that the proportion of M1-type macrophages was higher in the low-risk group, while the proportion of M2-type macrophages was higher in the high-risk group. M1 macrophages induce Th1-type immune responses, possess the ability to promote inflammation and anti-tumor immune activity, and can also produce reactive oxygen and nitrogen species to phagocytose and kill tumor cells (Arnold et al., 2014; Pan et al., 2020). M2-type macrophages can secrete pro-angiogenic factors such as vascular endothelial growth factor (VEGF) to promote tumor angiogenesis; they can also facilitate tumor cell invasion and metastasis by degrading various collagens and other extracellular matrix components (Annamalai et al., 2018; Zhu et al., 2021). These differences likely contribute to the prognostic disparities between risk groups.

Genomic mutation profiling analysis revealed distinct mutational landscapes between high- and low-risk groups. The high-risk group exhibited the highest frequency of PTPRD mutations. PTPRD, which encodes protein tyrosine phosphatase receptor type D, regulates cellular signaling and plays critical roles in cell growth, differentiation, migration, and adhesion (Yu et al., 2017b). Mutations in PTPRD can activate downstream JAK2/STAT3 signaling pathways, thereby promoting tumor growth (Veeriah et al., 2009), which may partially explain the poorer prognosis of the high-risk group. Differences in tumor mutational burden (TMB) and mutational allele tumor heterogeneity (MATH) were observed between groups, with the high-risk group showing higher TMB and MATH, both of which correlate with worse prognosis.

The results of the drug sensitivity analysis showed that the low - risk group exhibited lower IC50 values for commonly - used therapeutic drugs except Alpelisib, indicating higher sensitivity to these drugs. This suggests that low-risk patients may derive greater benefit from standard therapies compared to high-risk patients, who may require higher drug doses or combination strategies to achieve optimal efficacy. The higher sensitivity of the high - risk group to Alpelisib may be related to the higher frequency of PIK3CA gene mutations in this group (Andre et al., 2019).

In this study, the high-expression group of TACR1 showed lower IC50 values in drug sensitivity analysis, indicating higher sensitivity to most drugs except Alpelisib and Fulvestrant. This suggests that high TACR1 expression may be associated with enhanced responsiveness of breast cancer cells to these medications. Correlation analysis further validated this finding, revealing a significant negative correlation between TACR1 expression and drug responsiveness (i.e., higher TACR1 expression was associated with lower IC50 values and greater drug sensitivity), which provides guidance for clinical medication selection.

However, this study has several limitations. First, it relies entirely on data from the TCGA database. Although external validation was performed using GEO datasets, results should be verified through additional clinical experiments. Second, a larger cohort of breast cancer patients is needed to validate the clinical predictive value of the nomogram. If possible, mechanistic studies should further analyze and validate how the identified target genes (and their corresponding perioperative anesthetic drugs) influence breast cancer progression.

5. Conclusion

In this study, we constructed a risk model based on perioperative anesthesia-related drug target genes (PARDTGs) and found that the model performed well in other validation cohorts. A nomogram was also developed for potential clinical application. Based on this model, patients were divided into high- and low-risk groups for prognostic analysis, immune infiltration analysis, and genomic analysis. In addition, drug sensitivity analysis was conducted to provide guidance for clinical medication.

Abbreviations

BC: Breast cancer; TCGA: The Cancer Genome Atlas Program; GEO: Gene Expression Omnibus; DEG: different expression genes; PARDTG: perioperative anesthsia-related drugs target genes; DE-PARDTG: differentially expressed perioperative anesthsia-related drugs target genes; ROC-AUCs: Receiver Operating Characteristic - Area Under the Curves; OS: Overall survival; UALCAN: The University of ALabama at Birmingham CANcer; GO: Gene Ontology; KEGG: Kyoto Encyclopedia of Genes and Genomes; PCA：Principal component analysis; BP: Biological Process; MF: Molecular Function; CC: Cellular Component; GDSC: Genomics of Drug Sensitivity in Cancer; RNA-seq: RNA sequencing; TMB: Tumor Mutational Burden; MATH: Mutant - Allele Tumor Heterogeneity; MAF: Mutation Annotation Format MEP：Megakaryocyte - Erythroid Progenitor; NKT：Natural Killer T cell; MSC：Mesenchymal Stem Cell; HSCs: hematopoietic stem cell; CD4+ Tem: effector memory T cells; CD4+ Tcm: central memory T cells.

Authors contributions

DMY and JJL contributed to the writing, reviewing, and editing of the manuscript and was responsible for figure preparation. WJM searched public databases and collected the data. YP, YCQ, TY, WKL, XHS and JYZ performed the data analysis. XTHL and LYL contributed to the data analysis. YNL and YCW provided the research concept, supervised the study, reviewed the manuscript, and offered technical support. All authors have read and approved the final version of the manuscript.

Fundings

This research was supported by the Liaoning Provincial Natural Science Foundation Joint Fund (Doctoral Research Start-up Project) (2023-BSBA-291).

CRediT authorship contribution statement

Dongmei Yu: Writing – original draft. **Jiajia Li:** Writing – review & editing, Writing – original draft. **Wenjing Ma:** Data curation. **Yue Pei:** Formal analysis. **Ying-chao Qi:** Software, Formal analysis. **Tong Yu:** Visualization. **Wenkai Li:** Visualization. **Xiaohan Sun:** Formal analysis. **Jingyan Zhang:** Visualization. **Xuantonghe Li:** Methodology. **Longyan Liang:** Resources. **Yunen Liu:** Writing – review & editing, Project administration, Conceptualization. **Yichen Wang:** Writing – review & editing, Supervision, Project administration, Methodology, Conceptualization.

Declaration of Competing Interest

The authors declare that they have no known competing financial interests or personal relationships that could have appeared to influence the work reported in this paper.

Acknowledgments

We thank the relevant staff and data from the TCGA, GEO database. Additionally, we would like to thank all the developers of the R programming package for selflessly sharing their code.

Appendix A. Supporting information

Supplementary data associated with this article can be found in the online version at doi:10.1016/j.compbiolchem.2025.108681.

Data availability

The TCGA-BRCA (The Cancer Genome Atlas-Breast Cancer) data used in this study can be downloaded from the website (https://www.cancer.gov/ccg/research/genome-sequencing/tcga). Survival data and clinical information can be obtained from the official UCSC Xena website (https://xena.ucsc.edu/). Validation set data can be accessed from the GEO website (https://www.ncbi.nlm.nih.gov/geo/), and drug sensitivity data can be obtained from the GDSC website.

References

Andre, F., Ciruelos, E., Rubovszky, G., Campone, M., Loibl, S., Rugo, H.S., Group, S.-S., 2019. Alpelisib for PIK3CA-Mutated, hormone Receptor-Positive advanced breast cancer. N. Engl. J. Med. 380 (20), 1929–1940. https://doi.org/10.1056/NEJMoa1813904.

Annamalai, R.T., Turner, P.A., Carson, W.F. t, Levi, B., Kunkel, S., Stegemann, J.P., 2018. Harnessing macrophage-mediated degradation of gelatin microspheres for spatiotemporal control of BMP2 release. Biomaterials 161, 216–227. https://doi.org/10.1016/j.biomaterials.2018.01.040.

Arnold, C.E., Whyte, C.S., Gordon, P., Barker, R.N., Rees, A.J., Wilson, H.M., 2014. A critical role for suppressor of cytokine signalling 3 in promoting M1 macrophage activation and function in vitro and in vivo. Immunology 141 (1), 96–110. https://doi.org/10.1111/imm.12173.

Ayoub, N.M., Jaradat, S.K., Al-Shami, K.M., Alkhalifa, A.E., 2022. Targeting angiogenesis in breast cancer: current evidence and future perspectives of novel Anti-Angiogenic approaches. Front. Pharmacol. 13, 838133. https://doi.org/10.3389/fphar.2022.838133.

Bashar, M.D.A., Begam, N., 2022. Breast cancer surpasses lung cancer as the most commonly diagnosed cancer worldwide. Indian J. Cancer 59 (3), 438–439. https://doi.org/10.4103/ijc.IJC_83_21.

Conejo-Garcia, J.R., Biswas, S., Chaurio, R., Rodriguez, P.C., 2023. Neglected no more: b cell-mediated anti-tumor immunity. Semin. Immunol. 65, 101707. https://doi.org/10.1016/j.smim.2022.101707.

Deng, X., Vipani, M., Liang, G., Gouda, D., Wang, B., Wei, H., 2020. Sevoflurane modulates breast cancer cell survival via modulation of intracellular calcium homeostasis. BMC Anesth. 20 (1), 253. https://doi.org/10.1186/s12871-020-01139-y.

Engelhard, V., Conejo-Garcia, J.R., Ahmed, R., Nelson, B.H., Willard-Gallo, K., Bruno, T. C., Fridman, W.H., 2021. B cells and cancer. Cancer Cell 39 (10), 1293–1296. https://doi.org/10.1016/j.ccell.2021.09.007.

Festa-Vasconcellos, J.S., Piranda, D.N., Amaral, L.M., Indio-do-Brasil, V., Koifman, S., Vianna-Jorge, R., 2012. Polymorphisms in cycloxygenase-2 gene and breast cancer prognosis: association between PTGS2 haplotypes and histopathological features. Breast Cancer Res. Treat. 132 (1), 251–258. https://doi.org/10.1007/s10549-011-1828-0.

Fultang, N., Illendula, A., Lin, J., Pandey, M.K., Klase, Z., Peethambaran, B., 2020. ROR1 regulates chemoresistance in breast cancer via modulation of drug efflux pump ABCB1. Sci. Rep. 10 (1), 1821. https://doi.org/10.1038/s41598-020-58864-0.

Gabrilovich, D.I., Ostrand-Rosenberg, S., Bronte, V., 2012. Coordinated regulation of myeloid cells by tumours. Nat. Rev. Immunol. 12 (4), 253–268. https://doi.org/10.1038/nri3175.

Global Burden of Disease Cancer, C., Fitzmaurice, C., Abate, D., Abbasi, N., Abbastabar, H., Abd-Allah, F., Murray, C.J.L., 2019. Global, regional, and national cancer incidence, mortality, years of life lost, years lived with disability, and Disability-Adjusted Life-Years for 29 cancer groups, 1990 to 2017: a systematic analysis for the global burden of disease study. JAMA Oncol. 5 (12), 1749–1768. https://doi.org/10.1001/jamaoncol.2019.2996.

Guha, P., Bandyopadhyaya, G., Polumuri, S.K., Chumsri, S., Gade, P., Kalvakolanu, D.V., Ahmed, H., 2014. Nicotine promotes apoptosis resistance of breast cancer cells and enrichment of side population cells with cancer stem cell-like properties via a signaling cascade involving galectin-3, alpha9 nicotinic acetylcholine receptor and STAT3. Breast Cancer Res. Treat. 145 (1), 5–22. https://doi.org/10.1007/s10549-014-2912-z.

Hiller, J.G., Perry, N.J., Poulogiannis, G., Riedel, B., Sloan, E.K., 2017. Perioperative events influence cancer recurrence risk after surgery. Nat. Rev. Clin. Oncol. 15 (4), 205–218. https://doi.org/10.1038/nrclinonc.2017.194.

Inada, T., Kubo, K., Shingu, K., 2011. Possible link between cyclooxygenase-inhibiting and antitumor properties of propofol. J. Anesth. 25 (4), 569–575. https://doi.org/10.1007/s00540-011-1163-y.

Kadantseva, K., Subbotin, V., Akchulpanov, R., Berikashvili, L., Yadgarov, M., Zhukova, L., Likhvantsev, V., 2024. The impact of inhalation versus total intravenous anesthesia on the immune status in patients undergoing breast cancer surgery: a double-blind randomized clinical trial (TeMP). Front. Oncol. 14, 1401910. https://doi.org/10.3389/fonc.2024.1401910.

Kim, H.J., Jeon, S., Lee, H.J., Bae, J., Ri, H.S., Hong, J.M., Yun, E.J., 2023. Effects of sevoflurane on metalloproteinase and natural killer group 2, member d (NKG2D) ligand expression and natural killer cell-mediated cytotoxicity in breast cancer: an in vitro study. Korean J. Anesth. 76 (6), 627–639. https://doi.org/10.4097/kja.23323.

Kravtsov, D.S., Erbe, A.K., Sondel, P.M., Rakhmilevich, A.L., 2022. Roles of CD4+ t cells as mediators of antitumor immunity. Front. Immunol. 13, 972021. https://doi.org/10.3389/fimmu.2022.972021.

Kwakye, A.K., Kampo, S., Lv, J., Ramzan, M.N., Richard, S.A., Falagan, A.A., Wen, Q.P., 2020. Levobupivacaine inhibits proliferation and promotes apoptosis of breast cancer cells by suppressing the PI3K/Akt/mTOR signalling pathway. BMC Res. Notes 13 (1), 386. https://doi.org/10.1186/s13104-020-05191-2.

Li, L., Liu, Z.P., 2021. Detecting prognostic biomarkers of breast cancer by regularized cox proportional hazards models. J. Transl. Med. 19 (1), 514. https://doi.org/10.1186/s12967-021-03180-y.

Lu, H.L., Wu, K.C., Chen, C.W., Weng, H.K., Huang, B.M., Lin, T.Y., Wang, Y.K., 2021. Anticancer effects of midazolam on lung and breast cancers by inhibiting cell proliferation and Epithelial-Mesenchymal transition. Life (Basel) 11 (12). https://doi.org/10.3390/life11121396.

Madrid-Paredes, A., Casado-Combreras, M.A., Perez-Ramirez, C., Segura-Perez, A.M., Chamorro-Santos, C., Vergara-Alcalde, E., Canadas-Garre, M., 2020. Association of ABCB1 and VEGFA gene polymorphisms with breast cancer susceptibility and prognosis. Pathol. Res. Pract. 216 (4), 152860. https://doi.org/10.1016/j.prp.2020.152860.

Misawa, K., Kanazawa, T., Misawa, Y., Imai, A., Uehara, T., Mochizuki, D., Mineta, H., 2013. Frequent promoter hypermethylation of tachykinin-1 and tachykinin receptor type 1 is a potential biomarker for head and neck cancer. J. Cancer Res Clin. Oncol. 139 (5), 879–889. https://doi.org/10.1007/s00432-013-1393-5.

Pan, Y., Yu, Y., Wang, X., Zhang, T., 2020. Tumor-Associated macrophages in tumor immunity. Front. Immunol. 11, 583084. https://doi.org/10.3389/fimmu.2020.583084.

Pohl, A., Kappler, R., Muhling, J., D, V.O.N.S., Berger, M., 2017. Expression of truncated Neurokinin-1 receptor in childhood neuroblastoma is independent of tumor biology and stage. Anticancer Res. 37 (11), 6079–6085. https://doi.org/10.21873/anticanres.12056.

Poto, R., Gambardella, A.R., Marone, G., Schroeder, J.T., Mattei, F., Schiavoni, G., Varricchi, G., 2022. Basophils from allergy to cancer. Front. Immunol. 13, 1056838. https://doi.org/10.3389/fimmu.2022.1056838.

Shi, Y., Du, L., Lin, L., Wang, Y., 2017. Tumour-associated mesenchymal stem/stromal cells: emerging therapeutic targets. Nat. Rev. Drug Discov. 16 (1), 35–52. https://doi.org/10.1038/nrd.2016.193.

Stacer, A.C., Fenner, J., Cavnar, S.P., Xiao, A., Zhao, S., Chang, S.L., Luker, G.D., 2016. Endothelial CXCR7 regulates breast cancer metastasis. Oncogene 35 (13), 1716–1724. https://doi.org/10.1038/onc.2015.236.

Tsou, P., Katayama, H., Ostrin, E.J., Hanash, S.M., 2016. The emerging role of b cells in tumor immunity. Cancer Res. 76 (19), 5597–5601. https://doi.org/10.1158/0008-5472.CAN-16-0431.

Tyznik, A.J., Verma, S., Wang, Q., Kronenberg, M., Benedict, C.A., 2014. Distinct requirements for activation of NKT and NK cells during viral infection. J. Immunol. 192 (8), 3676–3685. https://doi.org/10.4049/jimmunol.1300837.

Varricchi, G., Galdiero, M.R., Loffredo, S., Marone, G., Iannone, R., Marone, G., Granata, F., 2017. Are mast cells MASTers in cancer? Front. Immunol. 8, 424. https://doi.org/10.3389/fimmu.2017.00424.

Veeriah, S., Brennan, C., Meng, S., Singh, B., Fagin, J.A., Solit, D.B., Paty, P.B., Rohle, D., Vivanco, I., Chmielecki, J., Pao, W., Ladanyi, M., Gerald, W.L., Liu, L., Cloughesy, T. C., Mischel, P.S., Sandor, C., Taylor, B., Schultz, N., Chae, T.A., 2009. The tyrosine phosphatase PTPRD is a tumor suppressor that is frequently inactivated and mutated in glioblastoma and other human cancers. Proc. Natl. Acad. Sci. USA 106 (19), 7822–7827. https://doi.org/10.1073/pnas.0900571106.

Wall, T., Sherwin, A., Ma, D., Buggy, D.J., 2019. Influence of perioperative anaesthetic and analgesic interventions on oncological outcomes: a narrative review. Br. J. Anaesth. 123 (2), 135–150. https://doi.org/10.1016/j.bja.2019.04.062.

Wang, J., Xu, J., Zheng, J., 2023. A1BG-AS1 promotes adriamycin resistance of breast cancer by recruiting IGF2BP2 to upregulate ABCB1 in an m6A-dependent manner. Sci. Rep. 13 (1), 20730. https://doi.org/10.1038/s41598-023-47956-2.

Wang, J., Zhang, X., Li, J., Ma, X., Feng, F., Liu, L., Wu, J., Sun, C., 2020. ADRB1 was identified as a potential biomarker for breast cancer by the co - analysis of tumor mutational burden and immune infiltration. Aging 13 (1). https://doi.org/10.18632/aging.202403.

Wang, H., Zhao, L., Wu, J., Hong, J., Wang, S., 2020. Propofol induces ROS-mediated intrinsic apoptosis and migration in triple-negative breast cancer cells. Oncol. Lett. 20 (1), 810–816. https://doi.org/10.3892/ol.2020.11608.

Wu, L., Lian, W., Zhao, L., 2021. Calcium signaling in cancer progression and therapy. FEBS J. 288 (21), 6187–6205. https://doi.org/10.1111/febs.16133.

Wu, J., Zhang, Y., Li, M., 2021. Identification of genes and miRNAs in paclitaxel treatment for breast cancer. Gynecol. Endocrinol. 37 (1), 65–71. https://doi.org/10.1080/09513590.2020.1822801.

Yang, N., Liang, Y., Yang, P., Yang, T., Jiang, L., 2017. Propofol inhibits lung cancer cell viability and induces cell apoptosis by upregulating microRNA-486 expression. Braz. J. Med. Biol. Res. 50 (1), e5794. https://doi.org/10.1590/1414-431X20165794.

Yang, L., Zhang, S., Pu, P., 2023. Comprehensive analysis of ACKR family members in breast cancer using prognostic values. Oncol. Lett. 26 (4), 425. https://doi.org/10.3892/ol.2023.14011.

Yu, T., Yang, G., Hou, Y., Tang, X., Wu, C., Wu, X.A., Liu, M., 2017. Cytoplasmic GPER translocation in cancer-associated fibroblasts mediates cAMP/PKA/CREB/glycolytic axis to confer tumor cells with multidrug resistance. Oncogene 36 (15), 2131–2145. https://doi.org/10.1038/onc.2016.370.

Yu, X., Zhang, F., Mao, J., Lu, Y., Li, J., Ma, W., Fan, S., Zhang, C., Li, Q., Wang, B., Song, B., Li, L., 2017. Protein tyrosine phosphatase receptor - type δ acts as a negative regulator suppressing breast cancer. Oncotarget 8 (58), 98798–98811. https://doi.org/10.18632/oncotarget.19286.

Zhang, D., Jia, T., Chen, X., Jiang, H., Guo, T., Dong, J., Yuan, Y., 2023. Bufalin reverses ABCB1-mediated resistance to docetaxel in breast cancer. Heliyon 9 (3), e13840. https://doi.org/10.1016/j.heliyon.2023.e13840.

Zhang, H., Liu, Y., Liu, J., Chen, J., Wang, J., Hua, H., Jiang, Y., 2024. cAMP-PKA/EPAC signaling and cancer: the interplay in tumor microenvironment. J. Hematol. Oncol. 17 (1), 5. https://doi.org/10.1186/s13045-024-01524-x.

Zhou, Y., Wang, M., Tong, Y., Liu, X., Zhang, L., Dong, D., Zhou, Y., 2019. miR-206 promotes cancer progression by targeting Full-Length Neurokinin-1 receptor in breast cancer. Technol. Cancer Res. Treat. 18, 1533033819875168. https://doi.org/10.1177/1533033819875168.

Zhu, S., Luo, Z., Li, X., Han, X., Shi, S., Zhang, T., 2021. Tumor-associated macrophages: role in tumorigenesis and immunotherapy implications. J. Cancer 12 (1), 54–64. https://doi.org/10.7150/jca.49692.